

ADAPTIVE DEADBEAT CONTROLLERS FOR BRUSHLESS DC DRIVES USING PSO AND ANFIS TECHNIQUES

Mohamed A. Awadallah^{*} — Ehab H. E. Bayoumi^{**}
— Hisham M. Soliman^{***}

The paper presents a tuning methodology for the parameters of adaptive current and speed controllers in a permanent-magnet brushless DC (BLDC) motor drive system. The parameters of both inner-loop and outer-loop PI controllers, which vary with the operating conditions of the system, are adapted in order to maintain deadbeat response for current and speed. Evenly distributed operating points are selected within preset regions of system loading. A particle swarm optimization (PSO) algorithm is employed in order to obtain the controller parameters assuring deadbeat response at each selected load. The resulting data from PSO are used to train adaptive neuro-fuzzy inference systems (ANFIS) that could deduce the controller parameters at any other loading condition within the same region of operation. The ANFIS agents are tested at numerous operating conditions indicating deadbeat response at all cases. The response of the developed controllers is compared to that of classical controllers whose parameters are tuned using the well-known Ziegler-Nichols method. Results signify the superiority of the proposed technique over the classical method.

Key words: brushless DC motors, adaptive control, deadbeat response, particle swarm optimization, neuro-fuzzy systems

1 INTRODUCTION

The brushless DC (BLDC) motor is a permanent-magnet synchronous machine supplied from a six-transistor inverter whose on/off switching is determined by the rotor position [1], [2]. There are no brushes or commutator. The system is becoming increasingly attractive in high-performance variable-speed drives since it can produce torque-speed characteristic similar to that of a permanent-magnet conventional DC motor while avoiding the problems of failure of brushes and mechanical commutation. In addition to the reduction in maintenance needs, the BLDC motor has low inertia, large power to volume ratio, and significant reduction in friction and noise as compared with the permanent-magnet conventional DC servo motor at the same output rating. However, all the above advantages are purchased at the price of high cost and more complex controller than that of the conventional motor.

Good armature current response is indispensable if BLDC motors are to have satisfactory driving performance. Many current control techniques have been developed, *eg*, vector control [3], predictive control [4], deadbeat control [5], and direct torque control [6]. Each approach has its own advantages and limitations. Classical controllers, however, suffer from the variation of electrical machine parameters such as armature resistance. The electrical parameters frequently vary with driving conditions, *eg*, variation of temperature and saturation phenomenon. Furthermore, possible variable loads result in

more severe parameter variations. Coupling the mechanical load to the motor shaft may cause the variation of inertia and viscous friction coefficients. The main control objective is to force the speed and/or current of a BLDC motor to follow its reference trajectories. With such parameter uncertainties, serious performance deviations will occur. Therefore, the robustness against machine parameter variations is an important issue to keep continual control performance all the time.

Many of the proposed approaches with regard to parameter uncertainties are based on Lyapunov's direct method to find a nonlinear control law to stabilize these systems [7] and [8]. The approaches attempt to find nonlinear state feedback laws that guarantee stability for all possible uncertainties. In addition to the abovementioned techniques, some methods are based on modified algebraic Riccati equation to derive linear controls for stabilizing linear uncertain systems [9]. The feedback linearization technique has been applied to the control of nonlinear plants such as induction and BLDC motors [10–12]. In [13], a robust H_∞ control of a drive system is solved in the framework of linear matrix inequalities (LMI) and Lyapunov theory-S procedure. Another very effective robust technique is the sliding-mode control, which can cope efficiently with system uncertainties [14] and [15]. However, a chattering problem may arise. Some of the publications mentioned above use state feedback robust controllers, which require the implementation of a lot of sensors. Accordingly, the technique becomes expensive, while failure may occur in some sensors. The problem can be allevi-

^{*} Electrical Power and Machines Department, University of Zagazig, Zagazig, Egypt, awadalla@ksu.edu; ^{**} Power Electronics and Energy Conversion Department, Electronics Research Institute (ERI), Cairo, Egypt, Currently on Leave to Yanbu Industrial College, Kingdom of Saudi Arabia, ehab-bayoumi@lycos.com; ^{***} Electrical Engineering Department, Faculty of Engineering, Cairo University, Egypt. hsoliman1@yahoo.com

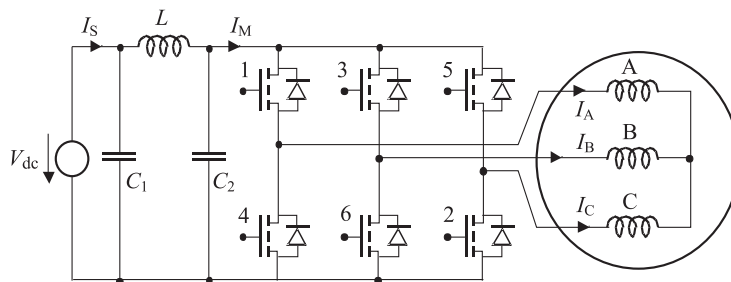


Fig. 2. Circuit diagram of the BLDC motor

The load torque is considered to vary with the motor speed. The proportionality factor relating load torque to shaft speed is taken as a nonlinear constant, which depends on the loading condition. Consequently, the load torque could be given as

$$T_L = K_T \omega. \quad (4)$$

Accordingly, the mechanical equation of the rotor is

$$T_e - T_L = J \frac{d\omega}{dt} + B\omega. \quad (5)$$

Substituting Equations (3) and (4) into Equation (5) yields

$$K_b i_a - K_T \omega = J \frac{d\omega}{dt} + B\omega \quad (6)$$

where,

- K_b = EMF constant of the motor, V s/rad (N m/A).
- ω = Mechanical speed of the rotor, rad/s.
- T_e = Electromagnetic torque developed by the motor, N m.
- T_L = Load torque, N.m.
- K_T = Load torque constant, N.m.s/rad.
- J = Moment of inertia of the motor shaft and attached load, kg m².
- B = Coefficient of friction, N m s/rad.

The time-domain equations given above yield the transfer functions shown in the block diagram of Fig. 1, which accounts also for the transfer functions of the inverter bridge, current transducer, and speed sensor.

2.2 Controller design

The cascade control system of the BLDC motor drive (Fig. 1) contains a current controller in the inner loop, and a speed controller in the outer loop. Both controllers are of the PI type; the parameters of both controllers are adapted to cope with the varying operating conditions of the system. The moment of inertia of the shaft and attached load, J , and the load torque constant, K_T , vary independently based on the conditions of the mechanical loading at the motor shaft. In addition, the effective value of the armature circuit resistance, R_a , changes with the load on the motor. The reason is that the stator current

of the motor increases with the mechanical load leading to an increase in the temperature rise due to copper loss. No other parameter of the system seems to change significantly with the operating conditions. In brief, the proportional and integral constants of both current and speed controllers should be tuned based on the J , K_T , and R_a parameters of the system.

The only varying system parameter, which appears within the inner current control loop, is the armature circuit resistance, R_a . Accordingly, the parameters of the current controller should be tuned solely based on R_a . Nevertheless, one distinct feature of the control system of the BLDC motor drive is the fact that the two controllers work at two different time scales.

The proposed technique of controller design relies on selecting a set of operating points uniformly distributed over a wide range. PSO is employed independently at each of the selected points in order to obtain the controller parameters which minimize the percentage overshoot of the step response to assure deadbeat behavior. The data attained from PSO algorithm is used to train an adaptive neuro-fuzzy inference system (ANFIS) that would deduce the controller parameters for deadbeat response at any point within the operating region. The ANFIS agent is trained off-line and will be implemented to adjust the controller parameters on-line as the operating conditions change. Therefore, the core of the adaptive current controller is an ANFIS module with one input denoting the effective armature circuit resistance, and two outputs representing the parameters of a PI controller. Similarly, the inputs to the ANFIS tool of the adaptive speed controller are the shaft moment of inertia and load torque constant, while the outputs signify the two parameters of the PI controller.

3 INTELLIGENT TOOLS

The present work makes use of the state-of-the-art paradigms of the modern artificial intelligence for optimization and adaptive inference. PSO is used to minimize the percentage overshoot of the system response in order to obtain deadbeat behavior. Neuro-fuzzy systems

are trained to infer the controller parameters at any operating condition other than those of the training data obtained via PSO.

3.1 Particle swarm optimization (PSO)

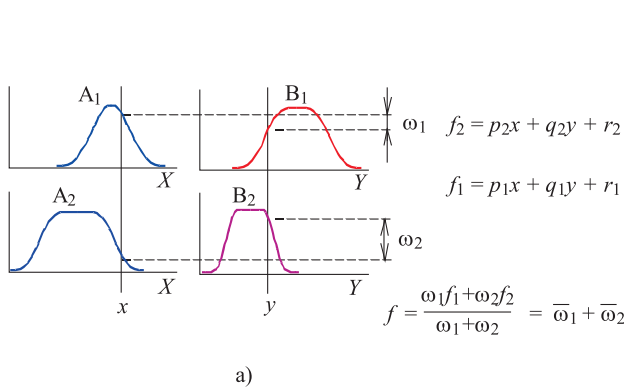
The PSO, which is a member of the evolutionary routines family, mimics the social behavior of a swarm of birds (particles) seeking the richest food source in a large field [19–24]. The algorithm exploits a population of randomly generated potential solutions in order to detect the global minimum of a highly nonlinear multimodal objective function. The PSO is a derivative-free algorithm, which utilizes cooperation, competition, and experience of the population individuals along with probabilistic transition rules of search.

The algorithm starts with a randomly generated population of individual particles representing potential solutions to the optimization problem. Each particle signifies a position in the search space, at which the objective function is evaluated. The particles move in the search space affected by three factors, namely, the previous movement of the same particle, the position of the best particle of the current population (local best), and the position of the best particle over the previous iterations (global best). The new velocities of the particles are probabilistically determined as given in Equation 7, while the new positions are computed as shown in Equation 8. One distinct attribute of PSO, compared to other evolutionary techniques, is that it does not employ the “survival of the fittest” concept as it does not implement a direct selection function. In other words, particles of low fitness can survive and probably visit any point in the search space.

$$v_i^{k+1} = wv_i^k + \alpha(P_l^k - x_i^k) + \beta(P_g^k - x_i^k), \quad (7)$$

$$x_i^{k+1} = x_i^k + v_i^{k+1} \quad (8)$$

where,



- v_i^{k+1} = the velocity vector of the i^{th} particle at the $(k+1)^{\text{th}}$ iteration,
- w = inertia weighting factor,
- v_i^k = the velocity vector of the i^{th} particle at the k^{th} iteration,
- α = bounded positive uniformly distributed random vector,
- P_l^k = the position vector of the local best particle at the k^{th} iteration,
- x_i^k = the position vector of the i^{th} particle at the k^{th} iteration,
- β = bounded positive uniformly distributed random vector,
- P_g^k = the position vector of the global best particle up to the k^{th} iteration,
- x_i^{k+1} = the position vector of the i^{th} particle at the $(k+1)^{\text{th}}$ iteration.

One evident advantage of PSO is the ease of implementation. Once the particle positions and velocities are randomly initialized, Equations 7 and 8 above are used to iterate on the fitness till convergence.

3.2 Adaptive neuro-fuzzy inference systems (ANFIS)

The adaptive neuro-fuzzy inference system (ANFIS) refers, in general, to an adaptive network which performs the function of a fuzzy inference system [25–29]. The most commonly used fuzzy system in ANFIS architectures is the Sugeno model since it is less computationally exhaustive and more transparent than other models. A consequent membership function (MF) of the Sugeno model could be any arbitrary parameterized function of the crisp inputs, most likely a polynomial. Zero and first order polynomials are used as consequent MF in constant and linear Sugeno models, respectively. In addition, the defuzzification process in Sugeno fuzzy models is a simple weighted average calculation. The fuzzy space is divided via grid partitioning according to the number of antecedent MF, and each fuzzy region is covered with a fuzzy rule. On the other hand, each fixed and adaptive node of the network performs one function or sub-function of the Sugeno model, as shown in Fig. 3, such

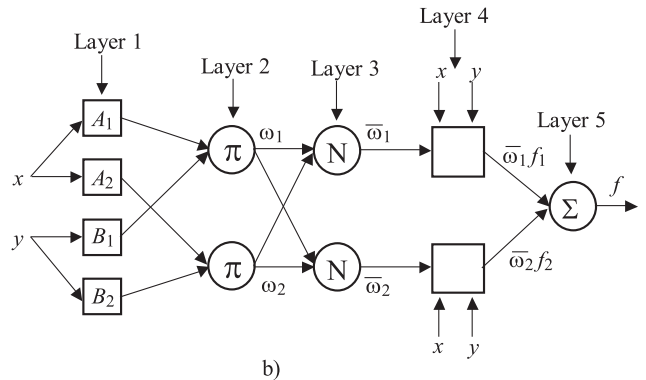


Fig. 3. (a) – Two-input, one-output, two-rule Sugeno model, (b) – equivalent ANFIS structure

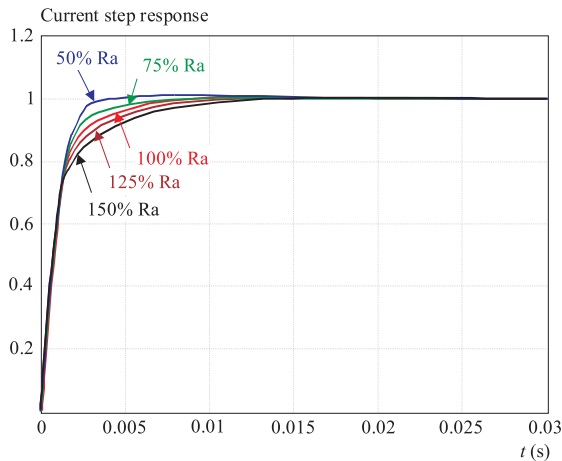


Fig. 4. Step response of the current with different controllers obtained from PSO

Table 1. Results of PSO optimization for the current controller.

R_a	K_p	K_i
50%	0.56	160.5
75%	0.58	198.21
100%	0.61	234.75
125%	0.64	265.89
150%	0.68	289.09

that the overall performance of the network is functionally the same as that of the fuzzy model.

The adaptive network employs an optimization algorithm to modify the parameters of the fuzzy inference system. The adaptation process aims at obtaining a set of parameters at which an error measure between the actual performance of the fuzzy model and a targeted set of training data is minimized. Classical optimization techniques, such as back propagation, could be used as well as hybrid algorithms. The total number of ANFIS modifiable parameters is a crucial factor of the computational effort required before the adaptation process is completed. Therefore, antecedent Gaussian MF, which is defined through two parameters only, is more preferable than other forms of MF. ANFIS combines the advantages of fuzzy systems and adaptive networks in one hybrid intelligent paradigm. The flexibility and subjectivity of fuzzy inference systems, when added to the optimization strength of adaptive networks, give ANFIS its remarkable power of modeling, learning, nonlinear mapping, and pattern recognition.

4 RESULTS

4.1 Current controller

The controller design scheme explained earlier is applied to both PI controllers of the current and speed loops of a BLDC drive system, whose parameters are given in Appendix 1. The parameters of the current controller are

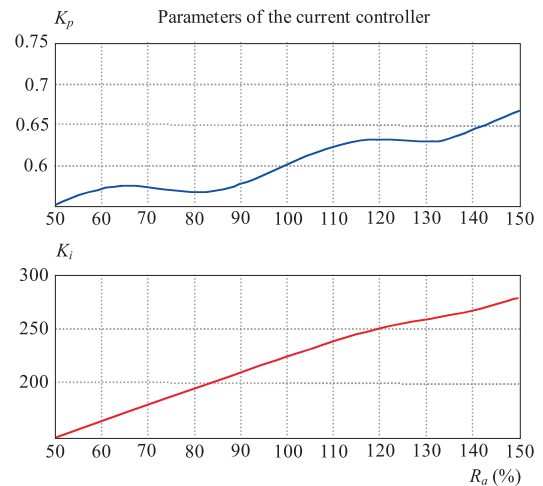


Fig. 5. Variation of current controller parameters against R_a as obtained from ANFIS

dependent on the effective value of the armature circuit resistance, R_a . A reasonably wide range of R_a is chosen to be between 50% and 150% of its nominal value [16]; such range accounts for large changes in the mechanical shaft load on the motor. Five uniformly distributed values of R_a are selected within the range, at which the plant transfer function of the inner loop is evaluated. PSO is run independently on the five cases to yield the PI controller parameters which maintain deadbeat step response of the system. The objective function to be minimized by PSO is given through Equation (9); the solution is rejected if the overshoot is not within $\pm 2\%$ as per the definition of deadbeat response [18]. The controller parameters obtained from PSO optimization are given in Table 1 against the corresponding values of R_a , while the step response of such cases is plotted in Fig. 4.

$$\min_{K_p, K_i} J_1 = \left| \frac{i_{a,\max} - i_{a,SS}}{i_{a,SS}} \right| \times 100. \quad (9)$$

The set of controller parameters obtained from PSO constitutes the training data of a single-input two-output ANFIS model, which signifies the heart of the adaptive current controller of the inner loop. The developed first-order Sugeno-type ANFIS has 3 Gaussian MFs per input. During the training phase of ANFIS, the mean square error stagnates at 2.7659×10^{-7} for K_p , and at 1.1194×10^{-4} for K_i when the system has been trained for 15 iterations. ANFIS training is accomplished using a hybrid adaptation routine based on the backpropagation and least square methods as offered in the Fuzzy Logic Toolbox of MATLAB®7.1. Testing of the trained ANFIS model involves creating a testing dataset via stepping on R_a from 50% to 150% by a step of 2%. It is evident that training data is a subset of the testing data. The 51 values of R_a are separately input to ANFIS to yield the corresponding parameters of the current controller. Values of the current controller parameters as obtained from ANFIS are plotted against the armature circuit resistance, R_a , in Fig. 5. Each value of R_a is used along

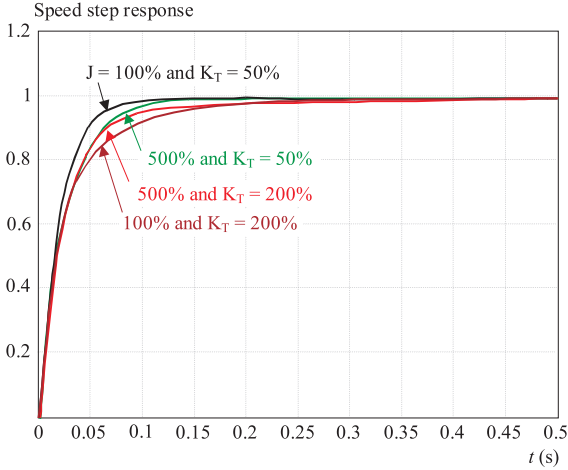


Fig. 6. Step response of the speed at selected loads with controllers obtained from PSO

Table 2. Results of PSO optimization for the speed controller.

J	K_T	K_p	K_i
100%	50%	0.057	0.58
	100%	0.059	0.96
	150%	0.061	1.26
	200%	0.063	1.49
200%	50%	0.0841	0.477
	100%	0.086	0.85
	150%	0.088	1.2
	200%	0.09	1.5
300%	50%	0.15	0.49
	100%	0.155	0.85
	150%	0.16	1.2
	200%	0.17	1.5
400%	50%	0.18	0.45
	100%	0.185	0.85
	150%	0.195	1.2
	200%	0.21	1.5
500%	50%	0.21	0.442
	100%	0.214	0.8
	150%	0.22	1.2
	200%	0.23	1.5

with its corresponding controller to find the step response of the current, of which the overshoot is computed. The percentage overshoot is zero at all points except for the 50% value of R_a , where the overshoot is 0.022%.

4.2 Speed controller

The same design procedures are repeated for the PI speed controller of the outer loop. The value of the armature circuit resistance, R_a , does not affect the performance of the outer loop since the current response is known to be much faster than the speed response. Therefore, R_a is fixed at its nominal value along with the corresponding current controller for all design steps of the speed controller. Consequently, the parameters of the speed controller should be tuned only with the moment

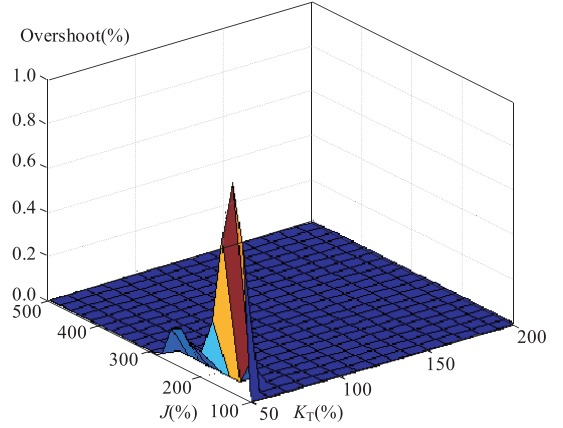


Fig. 7. Percentage overshoots of the speed step response at different loads

of inertia, J , and the load torque constant K_T , which vary independently. The shaft moment of inertia, J , is varied between 100% and 500% [2] with a step of 100% of the nominal value, while the load torque constant, K_T , is changed from 50% to 200% [2] with a step of 50% of the nominal value. Combining the 5 values of J with the 4 values of K_T results in a grid of 20 equally spaced load points spanning a satisfactorily wide range of operation. PSO is run independently to minimize the objective function given in Equation (10) at such 20 load points. The parameters of the PI speed controller, which yield deadbeat response, are saved at each loading condition. The controller parameters obtained from PSO are listed in Table 2, while the step response of the speed is shown in Fig. 6 at selected extreme load points. It should be noticed from Figs. 4 and 6 that the current response is at least 10 times faster than the speed response. Such observation validates the presumption that the R_a value does not affect the performance of the speed control loop.

$$\min_{K_p, K_i} J_2 = \left| \frac{\omega_{\max} - \omega_{SS}}{\omega_{SS}} \right| \times 100. \quad (10)$$

The parameters of the speed controller obtained from PSO are used to train an ANFIS module in order to deduce the parameters at any loading condition within the predetermined region. The first-order Sugeno-type ANFIS has two inputs and two outputs with 4 Gaussian MFs per input. After training ANFIS with the hybrid algorithm for 20 iterations, the mean square error reached a minimum of 6.17×10^{-3} and 6.62×10^{-3} for K_p and K_i , respectively. ANFIS design, training, and testing are completed using the Fuzzy Logic Toolbox of MATLAB®7.1. The testing dataset is composed by stepping on J from 100% to 500% with a step of 20% of the nominal value, and on K_T from 50% to 200% with a step of 10%. The 21 values of J are combined with the 16 values of K_T to yield 336 load points evenly distributed over the whole operating region. It is intuitive that the training data is a subset of the testing data.

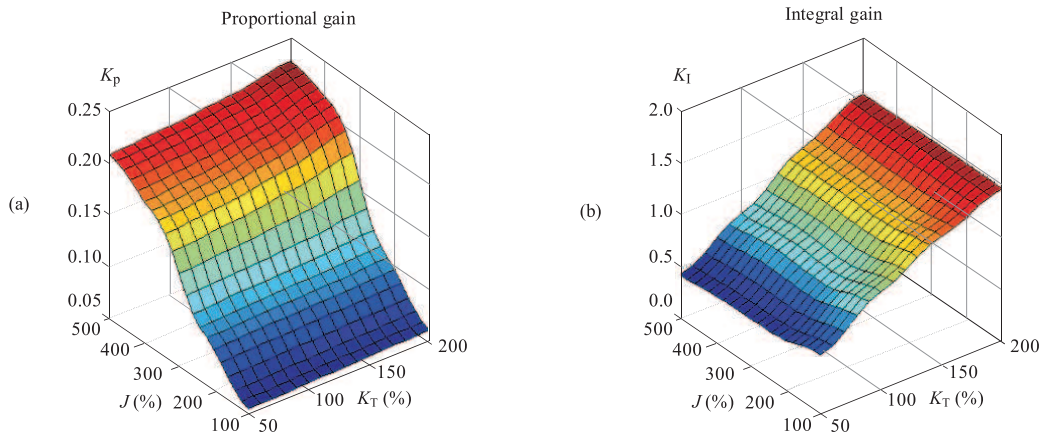


Fig. 8. Variation of speed controller parameters with loading conditions as obtained from ANFIS

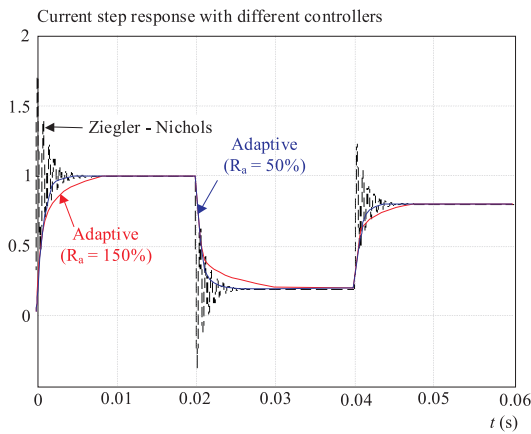


Fig. 9. Step response of the current using classical and proposed controllers

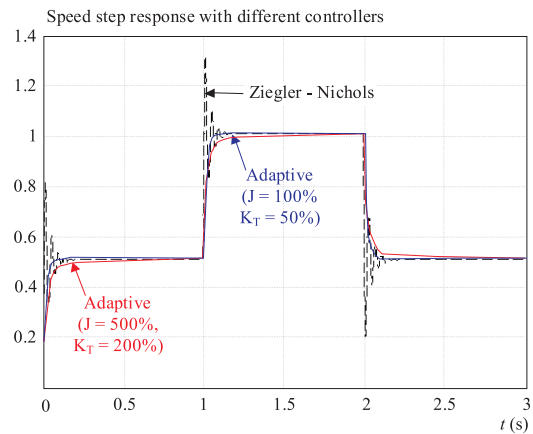


Fig. 10. Step response of the speed using classical and proposed controllers

The load points of the 336 testing cases are passed on to the ANFIS agent to obtain the corresponding parameters of the speed controller. Each load point is used along with its associated controller to compute the step response of the system. The nominal value of R_a and its subsequent current controller are used in the inner loop for all cases as pointed out earlier. Testing results of the developed ANFIS denote that the percentage overshoot at all testing points is always less than 1% indicating deadbeat response. Variation of the percentage overshoot versus operating conditions is shown in Fig. 7, while the relationship between parameters of the speed controller and operating conditions is depicted in Fig. 8. It should be emphasized that the percentage overshoot of the speed response is zero at the majority of the testing cases excluding some points with small J and K_T , where it does not exceed 1% (Fig. 7). Results of ANFIS testing validate the design methodology adopted in the paper and demonstrate its effectiveness to ensure the deadbeat response, which is exceedingly sought in high performance applications.

4.3 Comparison with classical controllers

The PI current and speed controllers are designed at nominal loading using the classical tuning routine of Ziegler-Nichols for the sake of comparison with the proposed adaptive controllers. The obtained proportional and integral constants of the PI current controller are 8.3125 and 9086, respectively. The current step response of the system is plotted in Fig. 9 in three cases: with the Ziegler-Nichols controller, and with the adaptive controller at 50% and 150% R_a . A unity step command in the current is applied at $t = 0$ seconds, followed by two other commands of -0.8 and 0.6 pu at $t = 0.02$ and $t = 0.04$ seconds, respectively. The responses evidently indicate the superiority of the proposed technique over classical method.

The same procedure is repeated for the speed controller, whose proportional and integral gains are found by Ziegler-Nichols technique to be 0.45 and 137, respectively. The step responses of the speed are plotted in Fig. 10 with the classical controller, and with the proposed controller at two extreme loading conditions. The step commands of 0.5, 0.5, and -0.5 pu are applied at

0, 1, and 2 seconds, respectively. The plots denote the superiority of the adaptive controller compared to the Ziegler-Nichols controller.

5 CONCLUSIONS

The paper presents a design technique for adaptive, deadbeat, PI current and speed controllers of BLDC motor drives using PSO and ANFIS paradigms. The system operating conditions, which influence the controller parameters are determined. PSO is utilized to obtain the parameters of both controllers, which maintain deadbeat response, at selected load points within the reasonably wide range of operation. Data resulting from PSO are used to train ANFIS agents to predict the controller parameters at different loads within the operating regions. Testing process of the developed controllers show that the deadbeat feature could be preserved for both current and speed responses within the specified region of operation. Finally, the proposed adaptive controllers are compared to classical controllers obtained through the well-known Ziegler-Nichols tuning method. The comparison shows the superiority of the proposed technique over classical tuning method.

Appendix 1 Parameters of the BLDC drive system

Motor Ratings and Parameters

Power	373 W
Current	17.35 A
Voltage	160 V
Torque	0.89 N.m
Armature resistance (R_a)	1.4 Ω
Armature inductance (L_a)	2.44 mH
Moment of inertia (J)	0.0002 kg.m ²
Coefficient of friction (B)	0.002125 N.m.sec/rad
EMF constant (K_b)	0.0513 V.sec
Transfer function parameters of system components	
Converter gain (K_r)	16 V/V
Converter time constant (T_r)	50 μ s
Current transducer gain (K_c)	0.288 V/A
Current transducer time constant (T_c)	0.159 ms
Speed sensor gain (K_w)	0.0239 V.sec
Speed sensor time constant (T_w)	1 ms

REFERENCES

- [1] CHIASSON, J.: Modeling and HighPerformance Control of Electric Machines, IEEE Press: Series on Power Engineering, John Wiley, 2005.
- [2] KRISHNAN, R.: Permanent Magnet Synchronous and Brushless DC Motor Drives: Theory, Operation, Performance, Modeling, Simulation, Analysis, and Design — Part 3: Permanent Magnet Brushless DC Machines and their Control, Virginia Tech, Blacksburg, 2000.
- [3] DAI, K.—LIU, P.—XIONG, J.—CHEN, J.: Comparative Study on Current Control for Three-Phase SVPWM Voltage-Source Converter in Synchronous Rotating Frame using Complex Vector Method, Proc. IEEE Power Electronics Specialists Conference (PESC'03) **2** No. 5 (2003), 695–700.
- [4] OH, I. H.—JUNG, Y. S.—YOUN, M. J.: A Source Voltage-Clamped Resonant Link Inverter for a PMSM using a Predictive Current Control Technique, IEEE Trans. on Power Electronics **14** No. 6 (1999), 1122–1131.
- [5] BOSE, B. K.: Power Electronics and Variable Frequency Drives, IEEE Press, New York, 1997.
- [6] YONG, L.—ZHUB, Z. Q.—HOWE, D.: Direct Torque Control of Brushless DC Drives with Reduced Torque Ripple, IEEE Trans. on Industry Applications **41** No. 2 (2005), 599–608.
- [7] CHEN, Y. H.: Design of Robust Controllers for Uncertain Dynamical Systems, IEEE Trans. on Automatic Control **55** No. 5 (1988), 487–491.
- [8] GUTMAN, S.: Uncertain Dynamical Systems: A Lyapunov Min-Max Approach, IEEE Trans. on Automatic Control **24** No. 3 (1979), 437–443.
- [9] TSAY, S. C.—FONG, I. K.—KUO, T. S.: Robust Linear Quadratic Optimal Control for Systems with Linear Uncertainties, Int. Journal of Control **53** No. 1 (1991), 81–96.
- [10] CHIASSON, J.: A New Approach to Dynamic Feedback Linearization Control of an Induction Motor, IEEE Trans. on Automatic Control **43** No. 3 (1998), 391–397.
- [11] OLIVIER, P. D.: Feedback Linearization of DC Motors, IEEE Trans. on Industrial Electronics **38** No. 6 (1991), 498–501.
- [12] KIM, K. H.—GAUIK, I. C.—CHUNG, S. K.—YOUN, M. J.: IEE Proc. on Electric Power Applications **144** No. 6 (1997).
- [13] LEE, M. N.—MOON, J. H.—JIN, K. B.—CHUNG, M. J.: Robust H_∞ Control with Multiple Constraints for the Track-Following System of an Optical Disk Drive, IEEE Trans. on Industrial Electronics **45** No. 4 (1998), 638–645.
- [14] UTKIN, V.—GULDNER, J.—SHI, J.: Sliding Mode Control in Electromechanical Systems, Taylor and Frances, New York, 1999.
- [15] BAYOUMI, E. H. E.—NASHED, M. N. F.: Fuzzy Sliding Mode Control for High Performance Induction Motor Position Drives, Journal of Power Electronics, KIPE, JPE vol 5 No. 1 (2005), 21–29.
- [16] BAYOUMI, E. H. E.—SOLIMAN, H. M.: PID/PI Tuning for Minimal Overshoot of Permanent-Magnet Brushless DC Motor Drive using Particle Swarm Optimization, Electromotion **14** No. 4 (2007), 198–208.
- [17] ASTROM, K. J.—WITTENMARK, B.: Adaptive Control, 2nd Edition, Pearson Education, 1995.
- [18] DORF, R. C.—BISHOP, R. H.: Modern Control Systems, 10th Edition, Prentice Hall, Upper Saddle River, New Jersey, 2005.
- [19] KENNEDY, J.—EBERHART, R.: Particle Swarm Optimization, Proc. IEEE Int. Conference on Neural Networks **4** (1995), 1942–1948.
- [20] EBERHART, R.—KENNEDY, J.: A New Optimizer using Particle Swarm Theory, Proc. Int. Symposium on Micro Machine and Human Science, 1995, pp. 39–43.
- [21] CLERC, M.—KENNEDY, J.: The Particle Swarm Explosion, Stability, and Convergence in a Multidimensional Complex Space, IEEE Trans. on Evolutionary Computation **6** (2002), 58–73.
- [22] PARSOPOULOS, K. E.—VRAHATIS, M. N.: Recent Approaches to Global Optimization Problems through Particle Swarm Optimization, Natural Computing I, Kluwer Academic Publishers, 2002, pp. 235–306.
- [23] ANGELINE, P.: Evolutionary Optimization versus Particle Swarm Optimization: Philosophy and Performance Differences, Evolutionary Programming VII, Springer-Verlag, 1998, pp. 601–610.
- [24] MENDES, R.—KENNEDY, J.—NEVES, J.: The Fully Informed Particle Swarm: Simpler, Maybe Better, IEEE Trans. on Evolutionary Computation **8** No. 3 (2004), 204–210.

- [25] JANG, J.-S. R. : ANFIS: Adaptive-Network-Based Fuzzy Inference System, *IEEE Trans. on Systems, Man, and Cybernetics* **23** No. 3 (1993), 665–685.
- [26] JANG, J.-S. R.—SUN, C.-T.—MIZUTANI, E. : *Neuro-Fuzzy and Soft Computing — A Computational Approach to Learning and Machine Intelligence*, Prentice-Hall, 1997.
- [27] JANG, J.-S. R.—SUN, C.-T. : Neuro-Fuzzy Modeling and Control, *Proceedings of the IEEE* **83** No. 3 (1995), 378–406.
- [28] JANG, J.-S. R. : Self-Learning Fuzzy Controllers Based on Temporal Back Propagation, *IEEE Trans. on Neural Networks* **3** No. 5 (1992), 714–723.
- [29] LIN, C.-T.—LEE, C. S. G. : Neural-Network-Based Fuzzy Logic Control and Decision System, *IEEE Trans. on Computers* **40** No. 12 (1991), 1320–1336.

Received 30 September 2008

Mohamed A. Awadallah was born in Zagazig, Egypt in 1971. He received the BS (with honors), and MS degrees from University of Zagazig, Egypt, in 1993 and 1997, respectively, and the PhD degree from Kansas State University, Manhattan, Kansas, USA, in 2004, all in Electrical Engineering. He is currently a lecturer with the Department of Electrical Power and Machines Engineering, University of Zagazig. His research interests include condition monitoring of electric machines and drives, power electronics, and artificial intelligence applications in power systems. Dr Awadallah is a member of Eta Kappa Nu, Tau Beta Pi, and Phi Kappa Phi.

Ehab H. E. Bayoumi obtained the BS from Helwan University, and MS from Ain Shams University, Egypt in 1988 and 1996, respectively. He earned his PhD from Cairo University, Egypt in collaboration with Lappeenranta University of Technology (LUT), Finland in 2001. He has been with Research Institute (ERI) Egypt since 1990. From 2000 to 2001 he joined LUT, Finland as a Visiting Researcher. He was appointed as an Assistant Professor at Chalmers University of Technology (CTH), Sweden from 2003 to 2005. He is an Associate Professor at ERI, Egypt. and currently on leave to Yanbu Industrial College (YIC), Kingdom of Saudi Arabia. His research interests include high performance ac machines, power quality, switching power converters, DSP-based control applications, and nonlinear control applications in power electronics and electric drive systems.

Hisham M. Soliman was born in Cairo Egypt in 1949. He received the BSc(with honors) and MSc degrees in Electrical Engineering from Cairo University, Egypt, in 1972 and 1975, respectively and the PhD in automatic control from the University of Paul Sababtier, Toulouse, France, in 1980. He is a Professor of Electrical Engineering at Cairo University, Cairo, Egypt. He served at the universities of: Saskatchewan, Canada; Garyounis, Libya; Emirates, UAE; and Yanbu industrial college, Kingdom of Saudi Arabia. His areas of research include Hierarchical/decentralized control of large-scale systems, robust control and power system control. He is a member of the Egyptian Engineering Syndicate.



EXPORT - IMPORT
of periodicals and of non-periodically
printed matters, books and CD-ROMs

Krupinská 4 PO BOX 152, 852 99 Bratislava 5, Slovakia
tel: ++421 2 638 39 472-3, fax: ++421 2 63 839 485
info@slovart-gtg.sk; <http://www.slovart-gtg.sk>

